Desalination and Water Treatment
www.deswater.com

doi: 10.5004/dwt.2020.26012

198 (2020) 376–385
September

Synthesis and characterization of TiO_2 and Ag/TiO_2 thin-film photocatalysts and their efficiency in the photocatalytic degradation kinetics of Orange G dyestuff

Derya Tekin[a,*], Taner Tekin[b], Hakan Kiziltas[b]

[a]*Department of Metallurgical and Materials Engineering, Faculty of Engineering, Ataturk University, Erzurum, Turkey, email: deryatekin@atauni.edu.tr (D. Tekin)*
[b]*Department of Chemical Engineering, Faculty of Engineering, Ataturk University, Erzurum, Turkey, emails: ttekin@atauni.edu.tr (T. Tekin), h.kiziltas@atauni.edu.tr (H. Kiziltas)*

Received 4 March 2019; Accepted 24 April 2020

ABSTRACT

The TiO_2 and Ag/TiO_2 solutions were prepared by the sol–gel method. The solutions were coated on the quartz tubes by using the dip-coating method. The produced TiO_2 and Ag/TiO_2 thin-film photocatalysts were characterized by using scanning electron microscopy–energy-dispersive X-ray spectroscopy, X-ray diffraction, X-ray photoelectron spectroscopy, and chronoamperometric measurements. The characterization results showed that the photocatalysts were successfully synthesized, and the Ag/TiO_2 thin-film photocatalyst had a higher photocurrent intensity than the TiO_2 thin-film photocatalyst. To eliminate the lack of literature in the kinetic study, the synthesized photocatalysts were examined on the degradation of the Orange G solution. The effects of initial dye concentration, temperature, and light intensity on the photocatalytic degradation kinetics of Orange G were investigated. The network kinetic model was applied to determine the appropriate kinetic model for the decomposition of Orange G with the produced photocatalysts. The network kinetic model was found to be the appropriate kinetic model for the degradation of Orange G using the TiO_2 and Ag/TiO_2 thin film photocatalysts. The calculated activation energies of the TiO_2 and Ag/TiO_2 thin film photocatalysts by using the result of the experiments are 20.02 and 16.16 kJ/mol, respectively. Besides, the general rate equations for each photocatalyst were specified.

Keywords: Thin-film photocatalyst; Degradation of dye; TiO_2; Ag/TiO_2; Orange G; Network kinetics

1. Introduction

Technology developed to meet increasing human needs adversatively affects the environment and water pollution [1]. Especially, the water pollution formed by the wastewater of textile industries is poisoning the global water resources. The decrease of clean water resources endangers the life of creatures. Because of this reason, many researchers focus on the treatment of wastewater with different types of thin-film photocatalyst such as TiO_2 [2], Mg–Al layered double hydroxide [3], etc.

Although the different type of materials can be used as a photocatalyst, TiO_2 is the most preferred semiconductor because of its cheapness [4], great chemical stability, and high photocatalytic activity [5]. Though TiO_2 is being used effectively as a photocatalyst, its interest in a commercial sense is gradually diminishing. Because it is very difficult to remove this photocatalyst from the solution medium. Some separation methods such as filtration have been used to remove the photocatalysts from the reaction media, but the losses of photocatalyst have not been eliminated. As a result, the photocatalytic activity decreases due to these

* Corresponding author.

losses of the amount of the photocatalyst. The best-found solution to overcome this problem is the use of thin-film photocatalysts [6]. The use of thin-film photocatalysts prevents the photocatalyst losses in the reaction medium and allows the photocatalyst to be easily removed from the reaction medium.

In addition to photocatalyst losses that cause the photocatalytic activity to decrease, there is a natural disadvantage in titanium dioxide. TiO_2 has a large bandgap of about 3.2 eV which prevents the absorption of visible light under solar irradiation [7]. Besides, the recombination of radiation-induced electrons and holes decreases its photocatalytic efficiency [8]. Many studies have attempted to overcome these disadvantages by doping different metals or oxide, such as Fe [9], Cu [10], Ag [11], and CuO [12]. Among these metals and oxides, TiO_2 is widely coupled with Ag, which might promote the generation of Schottky barriers of the Ag/TiO_2 contact region. The formation of Schottky barriers prevents the electron-hole recombination and consequently increases the photocatalytic activity of TiO_2 [13].

Textile industries have used different types of dyes. The majority of dyes used in the textile industry are azo dyes, which have one or more azo bonds (–N≡N–). Orange G has frequently been used in textile dyeing processes [14].

In this study, the solutions of TiO_2, and Ag/TiO_2 thin film photocatalysts, which were prepared by the sol–gel method, were coated on the quartz tubes by the dip-coating method. The obtained photocatalysts were characterized by scanning electron microscopy (SEM) for the determination of surface morphology, energy-dispersive X-ray spectroscopy (EDS) for the definition of elemental analysis, X-ray photoelectron spectroscopy (XPS) for the surface elemental composition and the chemical states, X-ray diffraction (XRD) for the analysis of crystal structures, and chronoamperometric measurements for the identification of photoelectrochemical properties. Orange G dye was chosen as a target pollutant due to its frequent use in the textile industry. To resolve the literature deficiency in the kinetic study and to determine the photocatalytic activity, the synthesized photocatalysts were examined on the decomposition of the Orange G solution.

2. Experimental

2.1. Materials

The used chemical materials for the synthesis of TiO_2 and Ag/TiO_2 photocatalysts are titanium(IV) isopropoxide (TIP, purity above 97%) silver nitrate (purity above 99%), acetic acid (purity above 99.7%), acetone (purity above 97%), ethanol (99.9% purity), and methanol (99.8% purity). Orange G dye was used for the photocatalytic experiments. All used chemicals were purchased from Sigma-Aldrich (Darmstadt, Germany).

2.2. Preparation of TiO_2 solution

The preparation procedure of the TiO_2 solution consists of two solutions. In the first solution, 39 mL of titanium(IV) isopropoxide was dissolved in 450 mL of ethanol under the magnetic stirring at 1,000 rpm for 1.5 h. The prepared second solution, containing 90 mL of acetic acid and 45 mL of pure water, was slowly added dropwise into the stirred first solution. After 3 h, 500 mL of solution was taken for use in the dip-coating process.

2.3. Preparation of Ag/TiO_2 solution

The preparation procedure of the TiO_2 solution is exactly applied in the preparation of the Ag/TiO_2 solution. Differently, 7.8 g of $AgNO_3$ was added in the second solution [15].

2.4. Coating of thin-films

Before the dip-coating procedure, quartz tubes to be coated were ultrasonically cleaned in acetone, methanol, ethanol, and deionized water successively, and dried in an air stream. The dip-coating procedure was similarly applied for each thin-film photocatalysts. The cleaned quartz tubes were immersed in the previously prepared thin film solutions at a rate of 10 cm/min and a 4° angle, withdrawn at the same rate without delay and pre-calcined for 10 min at 125°C in an oven. The coating process was repeated 10 times. The calcination temperatures of the coated photocatalysts were determined using the calcination temperatures given in the literature. The calcination of thin-film TiO_2 and Ag/TiO_2 photocatalysts was carried out at 500°C to form the anatase phase [16,17]. The amount of coated photocatalyst on the quartz tube was about 13.58 mg.

2.5. Experimental system

The prepared thin-film photocatalysts (the area of coated quartz tubes is approximately 30 cm^2) were used for photocatalytic degradation of the Orange G dye. As shown in Fig. 1, the photocatalytic degradation of Orange G was carried out using a photocatalytic reactor. The reactor temperature was kept constant at the desired temperature with a programmable water circulator. The saturated O_2 concentration in the reaction medium was provided by an air pump. To investigate the effect of dye concentration, temperature, and light intensity, the different values of dye concentration (20, 30, 35, and 40 ppm), temperature (20°C, 30°C, 40°C, and 50°C) and light intensity (44, 88, and 132 W/m^2) were used in the experiment. For the quantitative analysis of Orange G concentration, roughly 3 mL of samples were withdrawn from the reaction medium, and their absorbance was measured by using UV-vis spectrophotometer at 474 nm (Evolution 500, Thermo). All experiments were carried out within 120 min.

2.6. Characterization

The crystal structures of the photocatalysts were examined by X-ray diffraction (XRD) (D/Max-2200, Rigaku, Japan). The surface morphologies of the prepared photocatalysts were investigated by using SEM and EDS (Inspect S50, Field Electron and Ion Company, Czech Republic). The surface elemental composition and the chemical states of the photocatalysts were characterized by XPS diffraction (Specs-Flex, Darmstadt, Germany). The linear sweep voltammetry experiments of the photocatalysts were carried out by VersaSTAT3 potentiostat system (Amedek, Ireland).

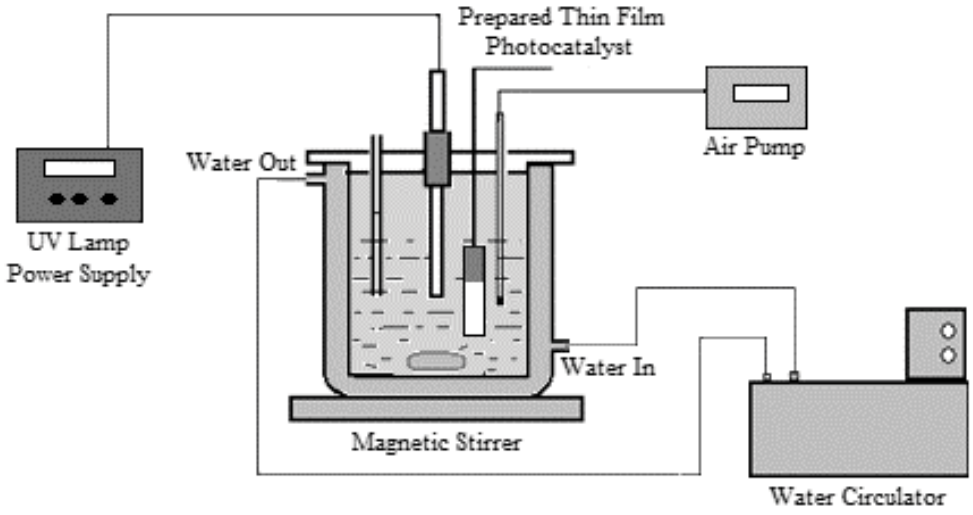

Fig. 1. Photocatalytic reactor system.

3. Results and discussion

3.1. XRD analysis

The XRD patterns of the TiO_2 and Ag/TiO_2 thin film photocatalysts are shown in Fig. 2. As shown in Fig. 2a, the most intense peaks of TiO_2 thin film photocatalyst belong to the anatase phase at the plane (111) at $2\theta = 40°$ and rutile phase at the plane (004) at $2\theta = 37.8°$. The anatase phase diffractions which have the angles of 25.28 in-plane of (101), 53.89 in-plane of (105), and 62.69 in-plane of (204) show conformity with 21-1272 JCPDS card number.

The XRD results of the Ag/TiO_2 thin film photocatalyst are shown in Fig. 2b. The XRD pattern of Ag/TiO_2 thin film has a similar XRD pattern of the TiO_2 thin film photocatalyst. Both the anatase and rutile phases were found in the XRD analysis. It is observed that the anatase phase which is crystallized is more and higher than the rutile phase. Depending on the amount of Ag added, non-dispersed Ag nanoparticles are observed at the angles of 38°, 66°, and 77°. In addition, the intensity of anatase peaks softly shrinks, and the intensity of rutile peaks slightly raises. These changes show that the crystallization of TiO_2 phases was impressed by the deposited Ag nanoparticles.

3.2. SEM and EDS analysis

Fig. 3a shows the SEM image of TiO_2 coated on the quartz glass surface. TiO_2 crystals have a spherical shape and measurable grain sizes are in the range of 155–214 nm. The nanoparticles do not have a homogeneous size distribution on the surface, and the emptiness between particles on the coated surface is observed prominently. The EDS result of the thin-film TiO_2 photocatalyst in Fig. 3b shows the presence of Ti and O in the catalyst. The presence of a low amount of carbon (C) in the sample indicates that there is some contamination on the surface of the catalyst. At the same time, the presence of Ti and O indicates the successful coating.

Fig. 3c shows the SEM image of Ag doped TiO_2 photocatalyst. The measured grain sizes are in the range of 80–160 nm. The Ag deposition on TiO_2 appears to result in grain size shrinkage compared to the SEM image of Fig. 3a. This shows that the large size TiO_2 nanoparticles and the small size Ag particles are synthesized. The EDS result of the Ag/TiO_2 photocatalyst shown in Fig. 3d shows the presence of Ti, O, and Ag in the photocatalyst. The presence of Ti, O, and Ag from the elementary analysis of the prepared thin-film photocatalyst is an indication of the successful coating process. The amount of Ag doped in TiO_2 is 2.31 wt.%.

3.3. XPS analysis

The XRD patterns of the Ag/TiO_2 thin film photocatalysts are shown in Fig. 4. As shown in Fig. 4a, the survey scan of the Ag/TiO_2 shows the presence of Ti, O, Ag, and C on the surface. The existence of C shows that there are some impurities. Figs. 4b–d show the high-resolution spectra of Ag 3d, Ti 2p, and O 1s, respectively. Although the binding energy of metallic silver ($3d_{5/2}$) was reported at 368 eV, the observed peaks at 368 and 374 eV can be ascribed to Ag $3d_{5/2}$ and Ag $3d_{3/2}$ of the metallic silver, respectively, as shown in Fig. 4b [18]. As shown in Fig. 4c, the observed peaks at 459 and 464.5 eV correspond to $2p_{3/2}$ and $2p_{1/2}$ of Ti^{4+} ions, respectively [19]. The Schottky junction between metallic Ag and TiO_2 can be proven by the shifted peak positions of the Ag 3d and Ti 2p [20]. The peaks at 530 and 531.5 eV, which is corresponding to O 1s, were associated with lattice oxygen and surface hydroxyl groups, respectively [21].

3.4. Linear sweep voltammetry analysis

In Fig. 5, the linear sweep voltammetry was carried out using the UV irradiation and dark medium. The measurements were carried out using periodic irradiation. The current value decreased to approximately zero in the dark medium. This is an indication that the current obtained under the UV irradiation is generated by the effect of UV irradiation. It can be concluded that the generated current is due to the photocatalytic activity of the photocatalyst and the charge transfer takes place very quickly. The current

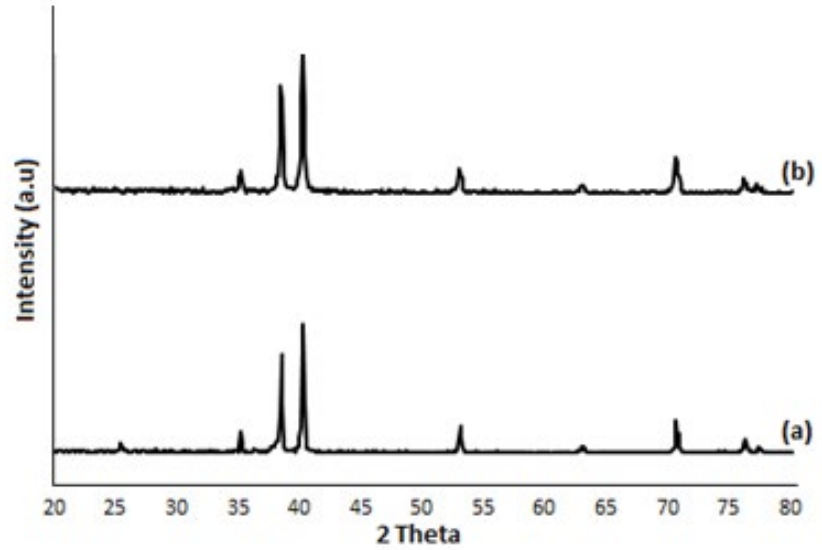

Fig. 2. XRD patterns of (a) TiO_2 and (b) Ag/TiO_2.

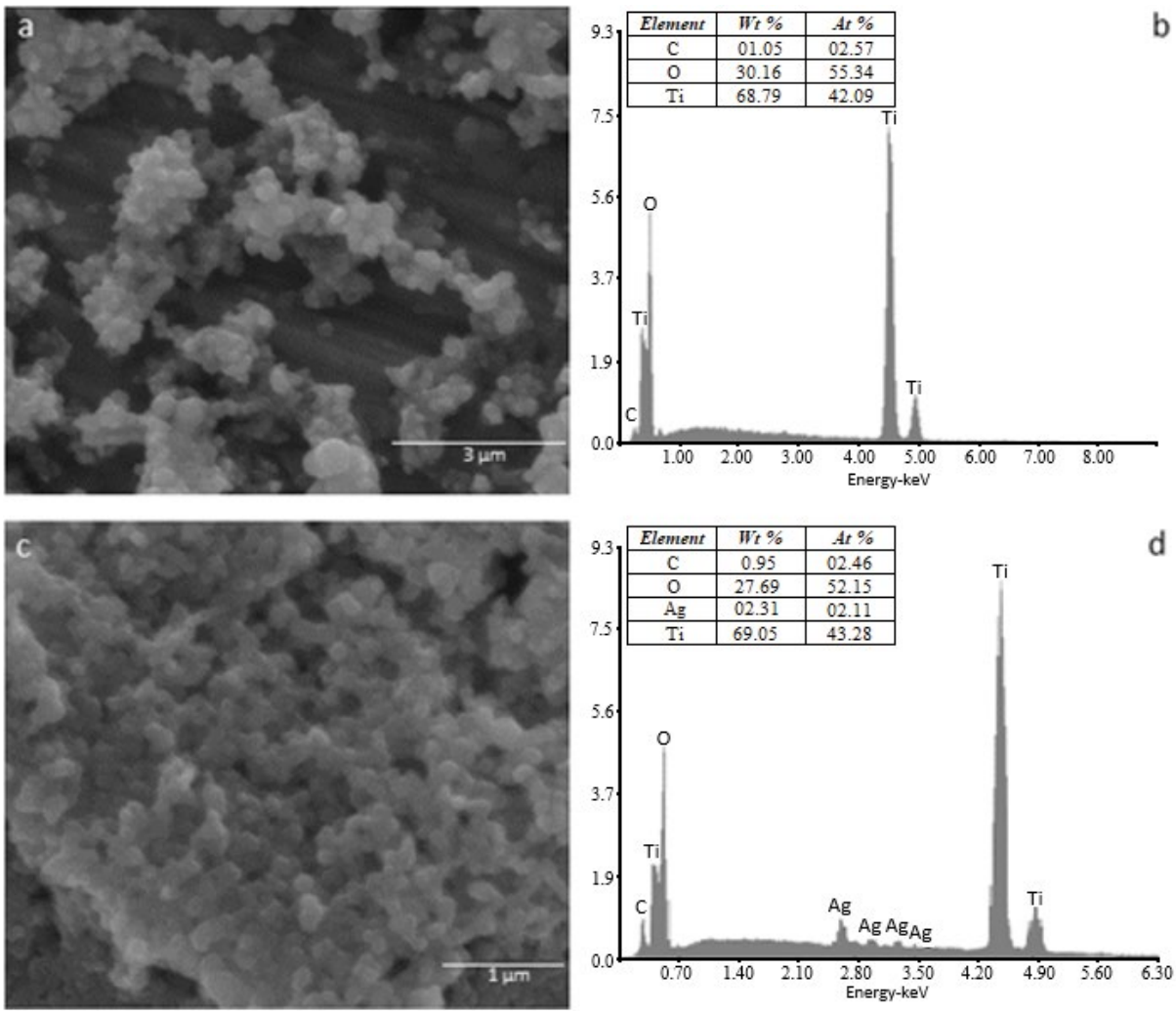

Fig. 3. SEM and EDS results of (a and b) TiO_2 and (c and d) Ag/TiO_2.

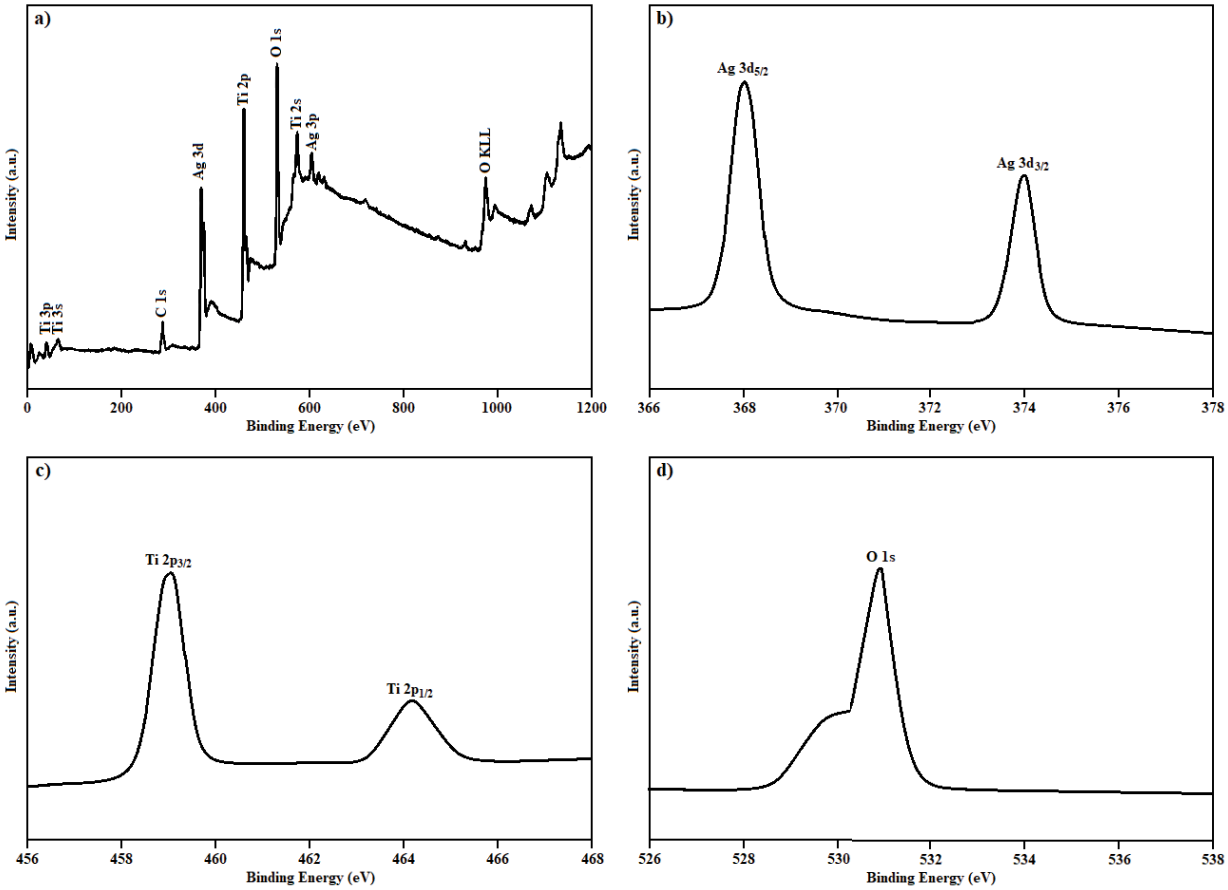

Fig. 4. XPS analysis: (a) survey spectrum of Ag/TiO_2; the high-resolution spectra of (b) Ag 3d, (c) Ti 2p, and (d) O 1s.

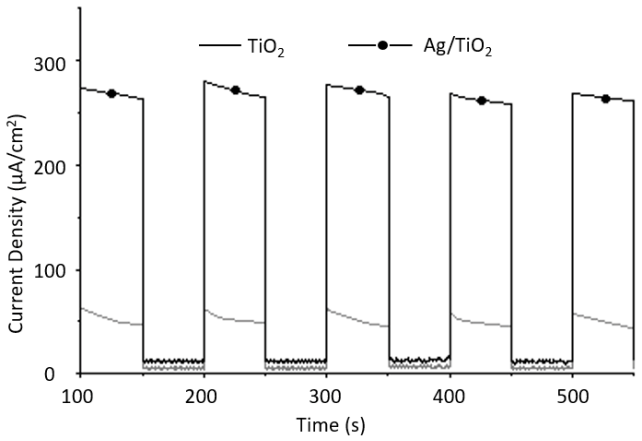

Fig. 5. Linear sweep voltammetry results of TiO_2 and Ag/TiO_2 photocatalyst.

density of the prepared thin film TiO_2 photocatalyst is approximately 50 μA/cm^2.

For the Ag/TiO_2 photocatalyst, the photocurrent formation is approximately 270 μA/cm^2 under UV irradiation; however, any current is not observed in the dark environment. A high increase in current density was observed when compared with the thin-film TiO_2 photocatalyst.

Ag deposition into TiO_2 nanomaterials has been demonstrated by previous studies that improve the separation of photo-generated electron-hole pairs and consequently prevent its recombination [21,22]. As shown in Fig. 6, after the Ag/TiO_2 nanomaterials were illuminated by UV light, the valance band (VB) electrons of TiO_2 were transferred to the conduction band (CB), and the holes were produced in VB. Because of the localized electric field at the interface of Ag/TiO_2 nanostructure, the transferred electrons of TiO_2 CB were mobilized to deposited Ag nanoparticles on the TiO_2. The electron transfers from Ag to TiO_2 were a remote possibility because the transfers are prevented by the Schottky barrier in the Ag/TiO_2 interface. Consequently, the electron-hole pairs were formed efficiently. The produced electron-hole pairs were reacted with O_2 and –OH and generated the hydroxyl and superoxide radicals which have an effective role in the decomposition of organic materials and charge transfer. Ag deposition on TiO_2 has a more effective production of electron-hole pairs compared to TiO_2. The Ag/TiO_2 photocatalyst showed higher current density than the TiO_2 photocatalyst because of more produced electron-hole pairs.

3.5. Kinetic model

When the TiO_2 photocatalyst is exposed to UV irradiation in an aqueous medium, hydroxide radicals are formed.

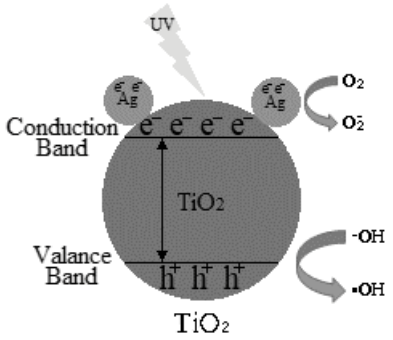

Fig. 6. Schematic diagram of electron-hole pairs separation of Ag/TiO_2 photocatalyst.

Hydroxyl radicals are strong oxidizing agents and act on organic compounds to form intermediate products. These intermediate products react with OH radicals to form the final products (P). Hydroxyl radicals can be consumed by inactive species. The photocatalytic degradation mechanism of dye solutions with TiO_2 photocatalyst is simply expressed as follows [23,24]:

$$TiO_2 + h\nu(\lambda < 390\ nm) \xleftrightarrow{k_1} TiO_2(e^-) + TiO_2(h^+) \quad (1)$$

$$TiO_2(h^+) + H_2O \xrightarrow{k_2} TiO_2(^{\bullet}OH) + H^+ \quad (2)$$

$$TiO_2(e^-) + O_2 \xrightarrow{k_3} TiO_2(^{\bullet}O_2^-) + H^+ \quad (3)$$

$$TiO_2(^{\bullet}OH) + C_{dye} \xrightarrow{k_4} Products + TiO_2 \quad (4)$$

$$TiO_2(^{\bullet}O_2^-) + C_{dye} \xrightarrow{k_5} Products + TiO_2 \quad (5)$$

It is accepted that the reaction step between the dye-adsorbed $OH^{\bullet}$ radicals (reaction 4) is determining the total reaction rate [25]. As a result, for the photocatalytic degradation of the dye, the following (Model-1) pseudo-first-order kinetic equation was obtained:

$$r_B = \left(\frac{-dC_{Dye}}{dt}\right) = k_P\left(C_{Dye}\right) \quad (6)$$

Since the pseudo-first-order kinetic model (Model-1) used for the degradation kinetics of dyes was not sufficient to define the kinetic data in various literature [8,26], the new kinetic model was given below (Model-2):

$$-\frac{dC_{dye}}{dt} = \frac{k_a C_{dye}}{\left(1 + k_b C_{dye}\right)} \quad (7)$$

where k_a and k_b are the constants of Model-2. This kinetic model called the network model was reported to be more appropriate for the kinetics of dye degradation [17,26].

The network kinetic model (Model-2) was used for the photocatalytic degradation of Orange G dye. Eq. (7) was integrated with the initial condition of $C_{dye} = C_0$ at $t = 0$ was obtained.

$$t = \frac{k_b}{k_a}\left(C_0 - C_{dye}\right) + \frac{1}{k_a}\ln\left(\frac{C_0}{C_{dye}}\right) \quad (8)$$

Eq. (8) was linearized and the following Eq. (9) was obtained. The model constants (k_a and k_b) were calculated, and the model compatibility was tested.

$$\frac{t}{\left(C_0 - C_{dye}\right)} = \frac{k_b}{k_a} + \frac{1}{k_a}\frac{\ln\left(C_0 / C_{dye}\right)}{\left(C_0 - C_{dye}\right)} \quad (9)$$

To determine whether Orange G dye is adsorbed on photocatalysts without photocatalytic effect, the experiments were repeated in the dark medium for each produced photocatalysts. The results showed that there was no decrease in the dye concentration due to adsorption on the catalyst surface and the values remained approximately constant. This situation showed that the reduction of dye concentrations in the experiments is only due to the photocatalytic decomposition.

In the photocatalytic degradation of Orange G dye with the TiO_2 and Ag/TiO_2 thin-film photocatalysts, $t/(C_0 - C_{dye})$ values were plotted against $\ln(C_0/C_{dye})/(C_0/C_{dye})$ values using the experimental parameters of initial dye concentration, temperature, and light intensity. The graphs, which were drawn for the temperature parameters, are given in Figs. 7 and 8. The model constants (k_a and k_b) were calculated using the intercept and slope values of the graphs and are given in Table 1. The linearity of the graphs shows the compatibility of the photocatalytic decomposition kinetics of Orange G dye to the Model-2 for all experimental parameters.

As can be seen from Table 1, it is determined that only the k_a model constant was changed with experimental parameters and the value of k_b remained constant. For the value of k_a, the following Eq. (10) can be used, which gives the variation of the rate constant in the literature with the model parameters [8,24,25].

$$k_a = \frac{k_o \exp\left(-Ea / RT\right) I_a}{1 + K_B C_{Do}} \quad (10)$$

where k_0 is a constant depending on temperature, E_a is the activation energy of the reaction, I_a is the light constant, K_B is the adsorption equilibrium constant, and C_{Do} is the initial dye concentration.

3.6. Effect of initial dye concentration on the kinetic model

As shown in Eq. (11), the reaction rate constant (k_a) derived using the Langmuir adsorption model is inversely proportional to the initial dye concentration. While the effect of initial dye concentration was studied in the experiments, all other parameters were kept constant ($T = 20°C$, $I = 44\ W/m^2$).

$$k_a \approx \left(\frac{k_1}{1 + K_B C_{Do}}\right) \quad (11)$$

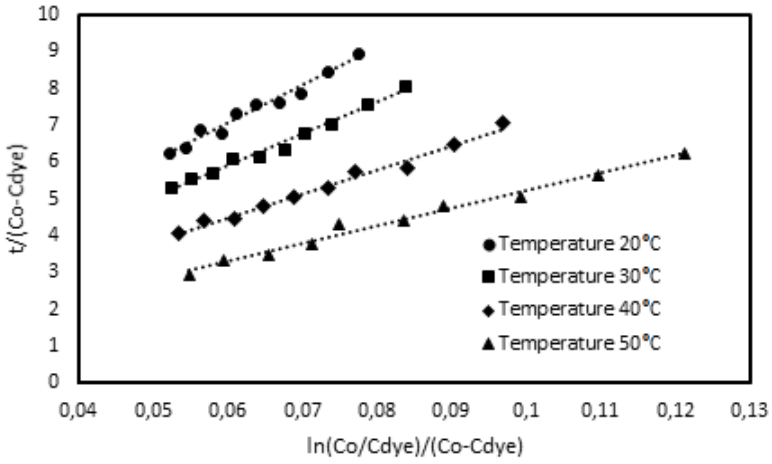

Fig. 7. Model-2 graph of degradation experiments of Orange G dye using TiO_2 thin-film photocatalyst for temperatures.

Table 1
The k_a and k_b model constants for the degradation experiments using TiO_2 and Ag/TiO_2 thin-film photocatalyst

	TiO_2 thin-film photocatalyst		Ag/TiO_2 thin-film photocatalyst	
Initial dye concentration (mg/L)	k_a model Constant (1/min)	k_b model constant (L/mg)	k_a model constant (1/min)	k_b model constant (L/mg)
20	0.00973	0.0086	0.0129	0.00971
30	0.00917	0.0087	0.0108	0.00994
35	0.00848	0.0086	0.0097	0.00962
40	0.00801	0.0087	0.0092	0.00991
Temperature (°C)				
20	0.00973	0.0086	0.0129	0.00971
30	0.0116	0.0084	0.0180	0.00972
40	0.0153	0.0086	0.0200	0.00924
50	0.0208	0.0085	0.0253	0.00966
Light intensity (W/m^2)				
44	0.00973	0.0086	0.0129	0.00971
88	0.0130	0.0084	0.0195	0.00975
132	0.0210	0.0085	0.0284	0.00980

where k_1 is a constant depending on the light intensity. When the equation was linearized was obtained.

$$\frac{1}{k_a} = \frac{1}{k_1} + \frac{K_B}{k_1} C_{Do} \tag{12}$$

In the photocatalytic degradation of Orange G using TiO_2 and Ag/TiO_2 thin-film photocatalysts, the k_a values, calculated values of 20, 30, 35, and 40 ppm initial dye concentrations, were used and the values of $1/k_a$ vs. the initial dye concentrations (C_{Do}) were plotted, and shown in Fig. 9. The adsorption equilibrium constant (K_B) value was calculated as 0.014 and 0.05 for TiO_2, and Ag/TiO_2, thin-film photocatalysts by using the intercept and slope values of the graphs, respectively.

3.7. Effect of temperature on the kinetic model

To calculate the activation energy of the photocatalytic degradation reaction of Orange G on the TiO_2 thin-film photocatalyst, the Arrhenius equation given below was used. As seen in Eq. (13), the reaction rate constant (k_a) was observed to be inversely exponential to the temperature. While the effect of temperature was studied in the experiments, all other parameters were kept constant (C_0 = 20 mg/L, I = 44 W/m^2).

$$k_a \approx k_2 \exp\left(-\frac{E_a}{RT}\right) \tag{13}$$

The values of $1/T$ vs. $\ln(k_a)$ were plotted using the k_a model constant values obtained from the photocatalytic

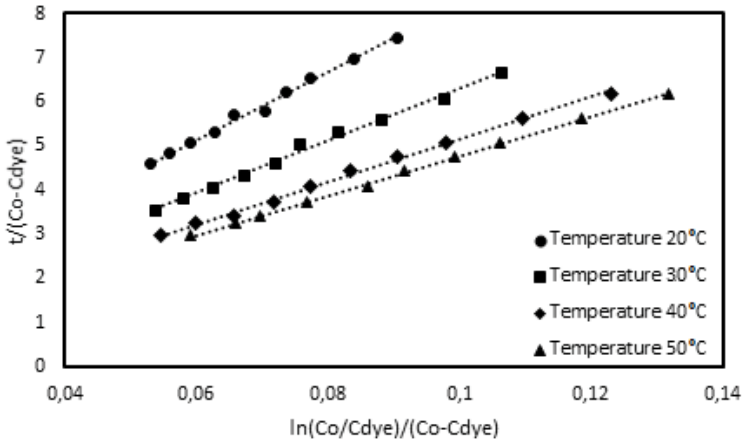

Fig. 8. Model-2 graph of degradation experiments of Orange G dyestuff using Ag/TiO_2 thin-film photocatalyst for temperatures.

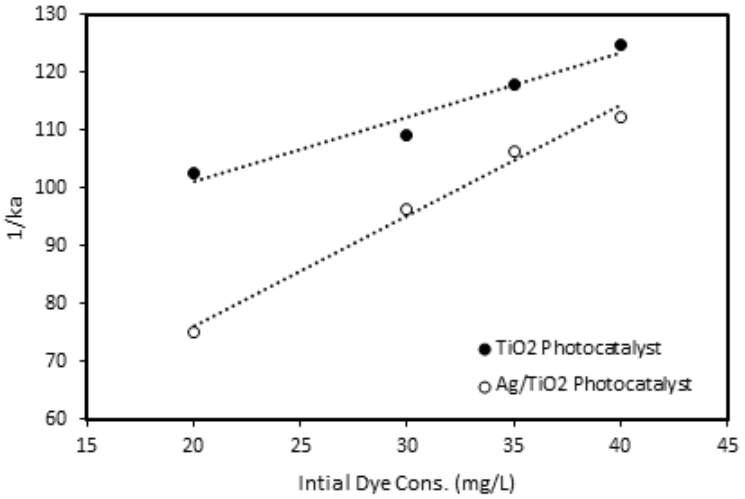

Fig. 9. Graph of the values of $1/k_a$ vs. the initial dye concentrations.

experiments performed to examine the effect of the temperature parameter, shown in Fig. 10. From the slope of the graph, the activation energies (E_a) of the decomposition reaction with the TiO_2 and Ag/TiO_2 thin-film photocatalysts were calculated as 20.02 and 16.16 kJ/mol, respectively.

3.8. Effect of light intensity on the kinetic model

While the effect of light intensity was studied in the experiments, all other parameters were kept constant (C_0 = 20 mg/L, T = 20°C). The light intensity (I_a) changes linearly with the k_a as seen from Eq. (10). In the photocatalytic degradation experiments of the Orange G dye using the TiO_2 thin-film photocatalyst, the values of k_a were plotted against the different light intensities (44, 88, and 132 W/m^2), shown in Fig. 11. Obtaining the linear curves in the graph shows the suitability of model-2.

The k_0 values in Eq. (10), giving the relationship between the k_a model constant and the experimental parameters, were calculated by using the Levenberg–Marquardt method and non-linear regression analysis. The values of k_0, calculated by statistical analysis, were determined as 0.97 ± 0.04 for the TiO_2 thin-film photocatalyst and 0.374 ± 0.02 for the Ag/TiO_2 thin-film photocatalyst.

The general rate equation given below was determined for the photocatalytic degradation kinetics of Orange G dye with the produced photocatalysts.

- The general rate equation for the decomposition reaction using the TiO_2 thin-film photocatalyst:

$$\frac{dC_{\text{dye}}}{dt} = \frac{0.907\text{I}_\text{a}\exp\left(-2409/T\right)}{1+0.014C_0}\frac{C_{\text{dye}}}{1+0.0086C_{\text{dye}}} \tag{14}$$

- The general rate equation for the decomposition reaction using Ag/TiO_2 thin-film photocatalyst:

$$-\frac{dC_{\text{dye}}}{dt} = \frac{0.374I_a\exp\left(-1944.8/T\right)}{1+0.05C_0}\frac{C_{\text{dye}}}{1+0.0097C_{\text{dye}}} \tag{15}$$

have been determined.

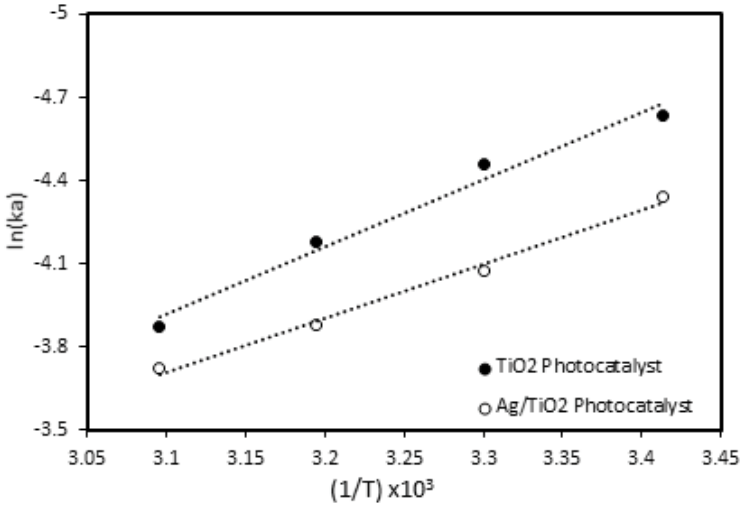

Fig. 10. Graph of the values of $1/T$ vs. $\ln(k_a)$.

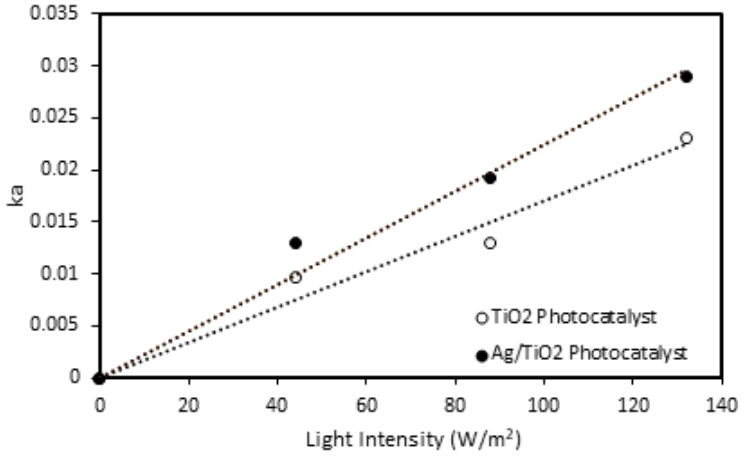

Fig. 11. Graph of the values of k_a vs. the light intensities.

4. Conclusions

The solutions of TiO_2 and Ag/TiO_2 thin film photocatalysts, which were prepared by the sol–gel method, were coated on the quartz tubes by the dip-coating method. The obtained photocatalysts were characterized by SEM–EDS, XRD, and chronoamperometry. To clarify the lack of literature in the kinetic study, the synthesized photocatalysts were examined on the degradation of the Orange G solution. The Ag/TiO_2 thin-film photocatalyst showed the most effective decomposition on Orange G. To determine the appropriate kinetic model for the decomposition of Orange G with the produced photocatalysts, the kinetic model of network (Model-2) was examined. Model 2 was determined as the most appropriate kinetic model for the decomposition of Orange G by using TiO_2 and Ag/TiO_2 thin-film photocatalysts.

Acknowledgments

This research was supported by the Scientific and Technological Research Council of Turkey (TÜBİTAK), Grant No: 214M658.

References

[1] H. Kiziltaş, T. Tekin, Increasing of photocatalytic performance of TiO_2 nanotubes by doping AgS and CdS, Chem. Eng. Commun., 204 (2017) 852–857.
[2] J. Singh, S.A. Khan, J. Shah, R.K. Kotnala, S. Mohapatra, Nanostructured TiO_2 thin films prepared by RF magnetron sputtering for photocatalytic applications, Appl. Surf. Sci., 422 (2017) 953–961.
[3] M.A. Elsayed, M. Gobara, S. Elbasuney, Instant synthesis of bespoke nanoscopic photocatalysts with enhanced surface area and photocatalytic activity for wastewater treatment, J. Photochem. Photobiol., A, 344 (2017) 121–133.
[4] A.J. Haider, R.H. Al-Anbari, G.R. Kadhim, C.T. Salame, Exploring potential environmental applications of TiO_2 nanoparticles, Energy Procedia, 119 (2017) 332–345.
[5] E. Al-Hetlani, M.O. Amin, M. Madkour, Detachable photocatalysts of anatase TiO_2 nanoparticles: annulling surface charge for immediate photocatalyst separation, Appl. Surf. Sci., 411 (2017) 355–362.
[6] R. Mechiakh, N.B. Sedrine, J.B. Naceur, R. Chtourou, Elaboration and characterization of nanocrystalline TiO_2 thin films prepared by sol–gel dip-coating, Surf. Coat. Technol., 206 (2011) 243–249.
[7] M.R. Delsouz Khaki, M.S. Shafeeyan, A.A.A. Raman, W.M.A.W. Daud, Evaluating the efficiency of nano-sized Cu doped TiO_2/

ZnO photocatalyst under visible light irradiation, J. Mol. Liq., 258 (2018) 354–365.
[8] D. Tekin, Photocatalytic degradation kinetics of Congo Red dye in a sonophotoreactor with nanotube TiO_2, Prog. React. Kinet. Mech., 39 (2014) 249–261.
[9] S.M.H. Al-Jawad, A.A. Taha, M.M. Salim, Synthesis and characterization of pure and Fe doped TiO_2 thin films for antimicrobial activity, Optik, 142 (2017) 42–53.
[10] F. Bensouici, M. Bououdina, A.A. Dakhel, R. Tala-Ighil, M. Tounane, A. Iratni, T. Souier, S. Liu, W. Cai, Optical, structural and photocatalysis properties of Cu-doped TiO_2 thin films, Appl. Surf. Sci., 395 (2017) 110–116.
[11] J. Singh, K. Sahu, A. Pandey, M. Kumar, T. Ghosh, B. Satpati, T. Som, S. Varma, D.K. Avasthi, S. Mohapatra, Atom beam sputtered Ag-TiO_2 plasmonic nanocomposite thin films for photocatalytic applications, Appl. Surf. Sci., 411 (2017) 347–354.
[12] J.F. de Brito, F. Tavella, C. Genovese, C. Ampelli, M.V.B. Zanoni, G. Centi, S. Perathoner, Role of CuO in the modification of the photocatalytic water splitting behavior of TiO_2 nanotube thin films, Appl. Catal., B, 224 (2018) 136–145.
[13] R. Zhou, S. Lin, H. Zong, T. Huang, F. Li, J. Pan, J. Cui, Continuous synthesis of Ag/TiO_2 nanoparticles with enhanced photocatalytic activity by pulsed laser ablation, J. Nanomater., 2017 (2017) 1–9.
[14] M. Vinayagam, S. Ramachandran, R. Vijayan, A. Sivasamy, Photocatalytic degradation of orange G dye using ZnO/biomass activated carbon nanocomposite, J. Environ. Chem. Eng., 6 (2018) 3726–3734.
[15] X.F. Lei, X.X. Xue, H. Yang, Preparation and characterization of Ag-doped TiO_2 nanomaterials and their photocatalytic reduction of Cr(VI) under visible light, Appl. Surf. Sci., 321 (2014) 396–403.
[16] D.J. Kim, S.H. Hahn, S.H. Oh, E.J. Kim, Influence of calcination temperature on structural and optical properties of TiO_2 thin films prepared by sol–gel dip coating, Mater. Lett., 57 (2002) 355–360.
[17] D. Tekin, Photocatalytic degradation of textile dyestuffs using TiO_2 nanotubes prepared by sonoelectrochemical method, Appl. Surf. Sci., 318 (2014) 132–136.
[18] P. Ramasamy, D.-M. Seo, S.-H. Kim, J. Kim, Effects of TiO_2 shells on optical and thermal properties of silver nanowires, J. Mater. Chem., 22 (2012) 11651–11657.
[19] J.F. Moulder, W.F. Stickle, P.E. Sobol, K.D. Bomben, Handbook of X-Ray Photoelectron Spectroscopy; Chastain, J, Perkin-Elmer Corp., Eden Prairie, MN, 1992.
[20] Z. Zhao, Y. Wang, J. Xu, Y. Wang, Mesoporous Ag/TiO_2 nanocomposites with greatly enhanced photocatalytic performance towards degradation of methyl orange under visible light, RSC Adv., 5 (2015) 59297–59305.
[21] T. Wang, J. Wei, H. Shi, M. Zhou, Y. Zhang, Q. Chen, Z. Zhang, Preparation of electrospun Ag/TiO_2 nanotubes with enhanced photocatalytic activity based on water/oil phase separation, Physica E, 86 (2017) 103–110.
[22] L. Liang, Y. Meng, L. Shi, J. Ma, J. Sun, Enhanced photocatalytic performance of novel visible light-driven Ag–TiO_2/SBA-15 photocatalyst, Superlattices Microstruct., 73 (2014) 60–70.
[23] A.L. Linsebigler, G. Lu, J.T. Yates, Photocatalysis on TiO_2 surfaces: principles, mechanisms, and selected results, Chem. Rev., 95 (1995) 735–758.
[24] I.K. Konstantinou, T.A. Albanis, TiO_2-assisted photocatalytic degradation of azo dyes in aqueous solution: kinetic and mechanistic investigations: a review, Appl. Catal., B, 49 (2004) 1–14.
[25] K.-T. Byun, H.-Y. Kwak, Degradation of methylene blue under multibubble sonoluminescence condition, J. Photochem. Photobiol., A, 175 (2005) 45–50.
[26] L.-A. Lu, Y.-S. Ma, M. Kumar, J.-G. Lin, Photochemical degradation of carbofuran and elucidation of removal mechanism, Chem. Eng. J., 166 (2011) 150–156.